Published in : Chemical Engineering Journal (2025), vol. 523
DOI: 10.1016/j.cej.2025.167966
Status : Postprint (Author's version)

BED CONFIGURATION EFFECTS OF TANDEM $ZnZrO_x$-BETA ZEOLITE CATALYSIS IN THE ONE STEP METHANOL-MEDIATED CO2 CONVERSION TO C4+ HYDROCARBONS

Foteini Lappa [a], Ibrahim Khalil [a,b], Grégoire Léonard [c,*], Michiel Dusselier [a,*]

[a] *Center for Sustainable Catalysis and Engineering (CSCE), KU Leuven, Leuven, B-3001, Belgium*
[b] *Université Claude Bernard Lyon 1, CNRS, IRCELYON, UMR 5256, Villeurbanne, F-69100 France*
[c] *Department of Chemical Engineering, Université de Liège, B6a Sart-Tilman, 4000, Liège, Belgium*
**Corresponding authors. E-mail addresses: g.leonard@uliege.be (G. Léonard), michiel.dusselier@kuleuven.be (M. Dusselier).*

Keywords:

Methanol to hydrocarbons ; Carbon dioxide Zeolite ; Tandem catalyst ; Proximity ; Paraffinic hydrocarbons

Abstract

The tandem system for CO_2 conversion to C4+ fuels through methanol as an intermediate, in one step, is studied in this work using $ZnZrO_x$ and beta zeolites. We show that the bed configuration is of major importance for such systems and highly dependent on the catalytic materials chosen. A dual bed configuration benefits the system showing the highest space time yield for C4+ paraffins when beta Si/Al = 15 is used (1.75 molC.kg_{cat}^{-1}.h^{-1}) and an impressive selectivity of 40 % to isobutane. More beta zeolites with different Si/Al are tested in both mixed and dual bed configuration and correlations between the catalytic behavior and the acidic properties of the zeolites are made. A hypothesis on a correlation between the position of the hydroxy species, especially the silanols, and the difference in activity due to different proximities is proposed, as zeolites with more external silanols seem to benefit more from a dual bed configuration. Higher temperatures and GHSVs increase the production of paraffins but simultaneously increase CO selectivity. Moreover, the tandem system is found stable for more than 30 h. These results are essential for the further development of tandem catalytic systems converting CO_2 to light alkanes.

1. Introduction

The catalytic hydrogenation of CO_2 is a very attractive technology that can potentially play a role in the global decarbonization efforts. Accounting for 77 % of Greenhouse Gas (GHG) emissions, CO_2 can be captured (Carbon Capture, CC technology) to be further stored (Carbon Capture and Storage, CCS technology) or used (Carbon Capture and Utilization, CCU technology). Hydrogen used for the realization of some of the CCU processes can be produced by multiple processes that have varying Global Warming Potential, the lowest of which can be achieved when hydrogen is produced by water

Published in : Chemical Engineering Journal (2025), vol. 523
DOI: 10.1016/j.cej.2025.167966
Status : Postprint (Author's version)

electrolysis if the electricity needed for this process is produced from renewable sources (11–48 g CO_2 eq/kWh) or nuclear plants (12 g CO_2 eq/kWh) [1]–[3]. Yet, the scaling of low emission H_2 is still a challenge.

Some appealing products resulting from CCU are hydrocarbons produced conventionally from refining or chemical industries such as olefins, paraffins and aromatics. Simpler products such as CO, CH_4 or methanol (MeOH) may be easier to achieve from CO_2 and thus are often used as intermediates for further conversion towards more complex compounds (in separate processes, or in one: tandem catalysis) [4]. Two main pathways have been studied differentiating based on the intermediate product. In the first one, the Reverse Water Gas Shift reaction (RWGS) is combined with Fischer-Tropsch synthesis to allow CO_2 to convert firstly to CO which is further converted to longer chain hydrocarbons (conventionally paraffins). In the second pathway, the methanol-mediated route, CO_2 is converted to methanol (CTM), and then methanol is converted to hydrocarbons (MTH) [5]-[7]. This process can have a variety of products depending on the carbon number and the nature of the carbon bonds, the selectivity towards which can be controlled by adjusting the second part of the process to Methanol to Olefins (MTO, using medium-small pores zeolites [8]-[9]), Methanol to Gasoline (MTG) or Methanol to Aromatics (MTA). The hydrogenation of CO_2 to MeOH is exothermic, whereas the hydrogenation of CO_2 to CO is endothermic:

$$CO_2 + 3H_2 \rightleftharpoons CH_3OH + H_2O \quad \Delta H^0_{298K} = -49.5 \text{ kj/mol} \qquad (1)$$

$$CO_2 + H_2 \rightleftharpoons CO + H_2O \quad \Delta H^0_{298K} = +41.2 \text{ kj/mol} \qquad (2)$$

It should be underlined that dimethylether (DME) is considered an important intermediate in the tandem reaction of CTM and MTH and is influenced by some of the same boundaries (exothermic, water formation and thus equilibrium issues) as CTM following the reaction [10]-[11]:

$$2CH_3OH \rightleftharpoons CH_3OCH_3 + H_2O \quad \Delta H^0_{298K} = -23.4 \text{ kj/mol} \qquad (3)$$

This reaction is acid-catalyzed, e.g. by γ-Al_2O_3, which shows high selectivity to DME due to its weak Lewis acidity and can restrict further (side) reactions. However, zeolites have also been intensively studied for this reaction because of their high content of acid sites, both Lewis and Brønsted (ZSM-5, Y, Beta, FER amongst others) [11]-[12].

MeOH as an intermediate is appealing because methanol itself is a liquid fuel (or energy dense molecule) and can also act as a precursor for versatile products (olefins, formaldehyde, gasoline, aromatics etc.) CTM can run at relatively low temperatures but needs increased pressures e.g. can reach a 60 % equilibrium yield at 90 bar and 200 °C (10 % equilibrium yield at 10 bar and 200 °C but approaching 0 % when the temperature increases to 300 °C), in comparison to RWGS reaction that can reach a maximum of 24 % equilibrium CO yield at 10 bar and 300 °C, based on previous studies and a H_2 to CO_2 ratio of 3 [13]. Many catalytic materials have been studied focusing on higher selectivity or yield of the intermediate (MeOH) with a focus on optimizing the tandem system from CO_2 to MeOH to hydrocarbon in one step. Some key catalysts for CO_2 to MeOH are the commercial Cu/ZnO/Al_2O_3, as well as In_2O_3 and $ZnZrO_x$ (also found in literature as ZnO-ZrO_2) [1]. $ZnZrO_x$ is a very interesting material due to the high MeOH selectivity and has been widely studied and characterized in literature, using in situ techniques, such as DRIFTS, showing the importance of the intermediate species (HCOO*) and the

Published in : Chemical Engineering Journal (2025), vol. 523
DOI: 10.1016/j.cej.2025.167966
Status : Postprint (Author's version)

type of the interfacial species (such as the hydroxyl groups Zn-OH-Zr) that have a strong effect in the mechanistic pathway and more specifically the extent of the hydrogen spillover and protonation of the main intermediates like formate [14]-[16]. For the tandem system, usually, an MTH catalyst is added to the system and more specifically a zeolite (or a zeotype) which can selectively alter the product distribution depending on the zeolitic properties such as topology, acidity or position of acid sites. The most typical zeolite applied for this reaction is ZSM-5 which was used for commercial MTG processes (Table S1) [17]. The combination of these materials that have different functions in "tandem", is of great importance, as it can alter the product distribution and enhance or weaken the intermediate reactions. Many factors contribute to this alteration, such as the amounts of each material, their positioning in the reactor and their proximity. The term 'proximity' can have a twofold meaning. More conventionally, and when discussing heterogeneous catalysis, with two types of catalytic sites, the term refers to the proximity of sites on a molecular level which can usually be altered during synthesis (or impregnation) leading to the synthesis of one catalytic bifunctional material [18]-[20]. Proximity can also refer to differentiated bed configurations, when two separate solid catalysts with each having a different type of sites, are used in tandem in a reactor. Focusing on the latter, it is usually challenging to find the key reason for explaining differences in the output when altering the bed configuration, as it is highly dependent on the specific materials and the reaction conditions because of the different kinetics and diffusion rates that are proved to alter the reaction outcome [21]. Bed configurations for two solid catalysts can be dual bed configuration (the two types of catalyst pellets placed in separate layers with or without an inert layer in between), physically mixed bed configuration (the two types of pellets mixed prior to placing the mixture in the reactor) or mortar mixed bed configuration (the two powdered materials placed in mortar and grinded together before making one type of pellets from the mixture and placing those in the reactor). Depending on the bed configuration, the products selectivity or reaction yields can be altered. In 2023, Parra et al. combined $ZnZrO_x$ with ZSM-5 zeolite (physically mixed) with the goal to convert a mixture of CO_2 and CO to gasoline range products, and it was found that at 420 °C, 50 bar, and $CO_2/CO_x = 0.5$ the C5+ yield (mainly isoparaffins C5 and C6) was almost 20.7 % with a CO_2 conversion of 39.7 % [22]. In 2020, Weber et al. showed that when combining Fe catalyst supported on alumina with sulfur and sodium promotors with ZSM-5 zeolite for the syngas conversion to hydrocarbons, the mortar mixed bed (powder mixing in mortar, closer proximity), was leading to an increase in methane selectivity and a decrease in the aromatics selectivity, versus all the other proximities (dual bed and physically mixed bed). In this case, this behavior was explained by the migration of the promotors (such as sodium) from the α-alumina supported Fe catalyst to the zeolite [23]. Studying the same reaction, Ding et al. tested ZnCrOx-SAPO and MnOx-SAPO catalysts in different proximities with different sizes of granules before mixing, and noticed that a closer proximity favored C2-C4 olefins compared to dual bed that showed higher selectivity to C2-C4 alkanes for both catalysts. The authors demonstrated that proximity effects are primarily influenced by the interaction that might be developed between the different active sites (e. g. CTM active sites from the oxide and Brønsted acid sites from the zeolite) as well as the role of the intermediates (e.g. ketene), the concentration of which can help to define the best proximity, in order to avoid mass transport limitations with the assumption that those species do not transform while transferring from the oxide to the zeolite. They concluded that when the catalysts lack easily migrating species (to the SAPO-34) such as in the case of MnOx, the reaction will benefit significantly from nanoscale proximity, hence concluding closer proximity is better. On the other hand, when the

Published in : Chemical Engineering Journal (2025), vol. 523
DOI: 10.1016/j.cej.2025.167966
Status : Postprint (Author's version)

migration of species occurs (as in the case of Zn species which can create Zn-OH upon contact with Brønsted acid sites), the yield of light olefins is enhanced by avoiding nanoscale proximity (granule size of 20 nm). Additionally, the acidity of the zeolites plays a crucial role, as controlling it can influence the dependency on proximity (weaker acidity reduces the influence a different proximity may have) [24]. A similar approach was shown by Lyu et al. for MTH reaction who compared different types of proximities. Beyond physical mixture and dual bed configuration, they tested core-shell proximity (another type of close proximity, the closest compared to the rest studied in this work), and presented that this closest proximity between γ-Al_2O_3 and ZSM-5 (γ-Al_2O_3 nanosheets around ZSM-5) resulted in higher MeOH conversion, C2-C3 olefins and aromatics selectivities [25]. More recently, Chen et al. studied this effect for CO_2 hydrogenation to olefins over a $ZnZrO_x$ and SSZ-13 in which it was shown that closer proximity of the functionalities enhances C2-C4 olefins production and CO_2 conversion while at the same time suppressing the CO selectivity. However, when the proximity was too close (0.3 nm, as measured by SEM and STEM), the effect was negative because of the decrease in area and volume of the micropores leading to higher CO selectivity and lower CO_2 conversion. The dual bed configuration in this case showed the highest selectivity to C2-C4 alkanes without drastically decreasing the CO_2 conversion [26]. Wang et al., studied an FeZnZr catalyst combined with ZSM-5 zeolite and showed that by increasing the proximity (from dual to core-shell) the hydrocarbon selectivity is enhanced and C1 components and aromatics are suppressed. At the same time, they showed the highest ratio of i-C5+/C5 + in the case of the core-shell configuration [27]. Dokania et al., showed that an InCo catalyst when combined with a Beta zeolite in a mixed bed configuration can result in higher CO_2 conversion and selectivity towards isoC4-C7, whereas when In@Co (Co_3O_4 and $In(OH)_3$ based on XRD before the reaction) is combined with Zn-Beta the opposite effect was noticed and a dual bed (separate layers) was more beneficial for that product cut. The latter was explained by the migration of Zn to the InCo catalyst in mixed bed case [28]. $ZnZrO_x$ and ZSM-5 as a tandem system was also studied by Li et al. showing that CO_2 conversion increased by increasing proximity, however when the two materials were grinded together (highest proximity studied by the group) the aromatics' selectivity was also the highest (as the conversion). When comparing a physical mixture and a dual bed configuration, the selectivity of the rest of the products stayed very close with only a slight increase in the selectivity of C5+ in the case of the dual bed configuration and less C2-C4 alkenes [29]. More recently, the system of $ZnZrO_x$ and ZSM-5 was studied by Parra et al. with the focus on production of isoparaffinic gasoline from CO/CO_2 mixture, and it was shown that the systems that benefited the reaction were those of closer proximity (physical mixing the 2 materials or bifunctional catalyst). The later (bifunctional catalyst) achieved the highest conversion of CO_2 and product yields [30]. Ghosh et al. studied the tandem reaction for the first time using a kinetic model (equilibrium was also taken into account) for a In_2O_3/ZSM-5 catalyst and were able to predict the experimental results [31]. A more specific research studying the migration effect in different proximities between multiple oxides and ZSM-5 was conducted by Wang et al. They showed that an important effect of protonic sites of the zeolite being neutralized by specific oxides derived species (In_2O_3 and ZnO), occurs for mortar mixed bed configuration (when the materials are grinded together in a mortar), leading to a decrease in BAS and more RWGS reaction products compared to dual bed configuration whereas other oxides such as ZrO_2 showed no migrating behavior [32].

Published in : Chemical Engineering Journal (2025), vol. 523
DOI: 10.1016/j.cej.2025.167966
Status : Postprint (Author's version)

It was shown in literature that the proximity effect is highly depending on the specific materials present in the system. Here, the bed configuration, more specifically, the proximity between the oxide catalyst (responsible for CTM) and the zeolite (responsible for MTH) was studied using $ZnZrO_x$ and Beta zeolites. Mixed bed configuration (a physical shaking of a mixture of oxide pellets and zeolite pellets) and dual bed configuration (separate layers of zeolite pellets topped by the oxide pellets) were used to demonstrate the proximity differences in the tandem system. As an effort to cover the gap for the combination of these specific materials and understanding the driving force for the optimum bed configuration, the correlation between the proximity of the 2 materials and the products selectivity was followed at various reaction conditions and was correlated to the specific materials' characteristics. The focus was put on the production of hydrocarbons in the light naphtha range, that could work as fuels and more specifically C4+ (including C4) hydrocarbons (alkanes and isoalkanes) and C5+ (including C5) hydrocarbons that are considered gasolinic compounds for the purposes of this work.

2. Experimental section

2.1. CHEMICALS

$ZrO(NO_3)_2 \bullet H_2O$ (Sigma Aldrich), $Zn(NO_3)_2 \bullet 6H_2O$ (Sigma Aldrich) and $(NH_4)_2CO_3$ (≥30.5 % NH_3, Carl Roth) were used as purchased. Zeolite Beta 12.5 (Clariant CZB 25), zeolite Beta 15 (Tosoh 930NHA, SiO_2/Al_2O_3 = 30), zeolite Beta 20 (Tosoh 940NHA, SiO_2/Al_2O_3 = 40), zeolite ZSM-5 40 (Zeolyst CBV 8014, SiO_2/Al_2O_3 = 80), zeolite Beta 75 (Clariant CZB 150) and zeolite Beta 250 (Tosoh 980HOA, SiO_2/Al_2O_3 = 500) were calcined before use to ensure or obtain the H form.

2.2. CATALYST PREPARATION

The $ZnZrO_x$ catalyst was synthesized following a procedure previously described using the solid solution method [14]. A solution is made by dissolving 15 g $ZrO(NO_3)_2 \bullet H_2O$ and 2.55 g $Zn(NO_3)_2 \bullet 6H_2O$ in 300 ml H_2O (deionized, Milli-Q, Merck, Synergy® UV system) under stirring and is labelled as solution (A). A second solution of 9 g $(NH_4)_2CO_3$ in 300 ml of H_2O (Milli-Q) is prepared and is labelled as solution (B). The solution (B) is added to the solution (A) dropwise at 70 °C, under vigorous stirring. The suspension was aged for 2 h under stirring at 70 °C and then was cooled down and washed several times with Milli-Q water and filtered by centrifugation. The sample was then dried at 100 °C for 48 h and calcined for 3 h at 500 °C (1 °C/min) in static air.

Zeolites were calcined at 550 °C in static air with a ramp of 1 °C/min for 6 h prior to being used experimentally.

Both oxides and zeolites were pelletized (under pressure 300–400 bar) prior to reaction and sieved to achieve pellets between 125 and 250 μm. In the case of mixed bed configuration, the weight of pelletized oxide and pelletized zeolite was added in a vial and was mixed manually by applying gentle shaking. In the case of dual bed configuration, the two types of pellets were carefully inserted in the

Published in : Chemical Engineering Journal (2025), vol. 523
DOI: 10.1016/j.cej.2025.167966
Status : Postprint (Author's version)

reactor by adding a layer of the zeolite and a layer of an oxide making sure the oxide was the first to come in contact with the gas feed (Fig. S1).

2.3. CATALYTIC TESTS

The tandem catalysis of CO_2 to C4+ linear hydrocarbons through MeOH was performed on a fixed bed stainless steel reactor with an inner diameter of 5 mm in a custom PID Eng&Tech catalytic unit. Prior to a typical experiment, the reactor was filled with 300 mg of catalysts (oxide: zeolite ratio of 1:1), and a leak test was performed at room temperature and a working pressure of 40 bar. The activation of the materials was performed in-situ, under working conditions (T = 300 °C and P = 40 bar), for 5 h, in the presence of the feed gases in high GHSV, ensuring very low conversion (< 1 %) but activation of the system (Fig. S3). Other activation ways were tested, using pure H_2 and pure N_2, leading to similar results but a slightly more intense conversion decrease (Fig. S2). The system was then switched to bypass mode, isolating the reactor, allowing the feed gases to be measured accurately in the GC, constituting the exact inlet flows of the experiment. Consequently, the unit was switched to reactor mode, allowing the feed gases to enter through the reactor, initiating the start of the reaction. The experimental conditions were T = 300 °C, P = 40 bar and 42.5 ml/min total feed of gases (5 ml/min N_2, 7.5 ml/min CO_2 and 30 ml/min H_2) with H_2:CO_2 = 4, unless mentioned otherwise. A typical experiment was conducted for 8 h unless mentioned otherwise. Three mass flow controllers were used to determine the inlet flows of the gases (two thermal mass flow controllers for N_2 and H_2 and a Coriolis mass flow controller for CO_2). The reactor and its tube oven are positioned inside a hotbox which is kept at 140 °C throughout the whole procedure and is connected with an online gas chromatograph (GC) with a heated line (150 °C). The GC (TraceGC 1300, G.A.S.) consists of one flame ionizing detector (FID) for the analysis of hydrocarbons C_1-C_{10} by a CP-Poraplot Q (CP7551) column and two thermal conductivity detectors (TCD) for the analysis of permanent gases principally by two Hayesep N, 60–80 columns, a Molsieve 5A, 60–80, a RT-XL Sulfur 60–80 and a SC-ST 60–80 columns.

The carbon balance was within an acceptable range of 97–101 %. It is important to note that when working in low conversions, the gap in the carbon balance can correspond to relatively high amounts of unknown carbon products (hydrocarbons or coke) or errors of the system as discussed in paragraph 3.2. For the purposes of this work, oxygenates are considered MeOH and DME, olefins are alkenes with a C2+ (including C2) chain length and paraffins are alkanes with C1+ (including C1) chain length (thus including CH_4 unless mentioned otherwise). The experimental results (product distribution, STY values etc.) presented in this paper correspond to one data point between the first 30–60 min of reaction, the reason being the slow decrease of conversion in later times. However, Time on Stream (TOS) results are presented in paragraph 3.2. The conversion of CO_2 (XCO_2,%), the space-time yield of the product i (STY_i, mol of C $kg_{cat}^{-1}.h^{-1}$) in terms of carbon number (CN_i) and molar flow ($\dot{n}$, $mol.h^{-1}$), the gas hourly space velocity (GHSV, $Nml.g_{cat}^{-1}.h^{-1}$) and the carbon balance (CB, %) were calculated using the formulas (4)– (7). In addition, for the calculation of the weight loss for the cokes and the water present on the zeolite after reaction, TGA was used, and then Eqs. (8)–(9) were applied to convert it in the desired expression.

Published in : Chemical Engineering Journal (2025), vol. 523
DOI: 10.1016/j.cej.2025.167966
Status : Postprint (Author's version)

$$X_{CO_2}(\%) = \frac{n_{CO_2 in} - n_{CO_2 out}}{n_{CO_2 in}} \times 100 \quad (4)$$

$$STY_i \left(molC\ kg^{-1}h^{-1}\right) = \frac{\dot{n}_i}{m_{cat}} \times CN_i \quad (5)$$

$$GHSV \left(Nml\ g_{cat}^{-1}h^{-1}\right) = \frac{\dot{V}}{m_{cat}} \quad (6)$$

$$CB\ (\%) = \frac{\sum (CN_i \times n_i)}{n_{CO_2 in}} \times 100 \quad (7)$$

$$Cokes \left(mol\ kg_{cat}^{-1}h^{-1}\right) = \frac{TGA\ Wloss}{Mr_{cokes} \times TOS \times m_{cat}} \quad (8)$$

$$Water \left(mol\ kg_{cat}^{-1}h^{-1}\right) = \frac{TGA\ Wloss}{Mr_{water} \times TOS \times m_{cat}} \quad (9)$$

where m_{cat} is the mass of the catalyst, $\dot{V}$ is the volumetric flow of feed gases ($Nml.h^{-1}$), CN_i, the carbon number of product i, Mr_{cokes} and Mr_{water}, the molar mass of cokes and water respectively and *TGA Wloss* the weight loss of the used catalyst as calculated from the TGA graph. It is worth noting that the choice of units for the STY_i is made to facilitate the direct comparison of products with different CN and it is expressed as mol of carbon of product i per kg of catalyst used and per hour of experiment (so 1 actual mol of propane produced per kg catalyst per hour would result in 3 mol of C $kg_{cat}^{-1}.h^{-1}$).

2.4. CHARACTERIZATION OF CATALYSTS

2.4.1. POWDER X-RAY DIFFRACTION (XRD)

To unravel the structure of the custom-made oxides, XRD measurements were conducted on a STOE STADI P Combi diffractometer in transmission mode operating at 20 kV. The scanning time was 10 min per sample and every sample was analyzed for an angle between the transmitted and the reflected beam in the range of 2θ of 0° to 60°. The X- ray inlet beams are monochromatic, focusing Ge(111) with Cu Ka radiation with wavelength, λ = 1.5406 Å (Fig. S4).

2.4.2. FOURIER-TRANSFORM INFRARED (FTIR) SPECTROSCOPY

To analyze the density of Brønsted and Lewis acid sites (BAS and LAS) of the zeolites, pyridine adsorption and desorption measurements followed with FT-IR spectroscopy were conducted. A Nicolet 6700 spectrometer equipped with a deuterated triglycine sulfate detector was used. Prior to the measurement, the zeolite powder was pressed into pellets with a density ranging between 5 and 20 mg per cm^2. The pellets were activated at 400 °C (5 °C/min) for 6 h in-situ under vacuum conditions (< 0.1 mbar). Post activation, a first FT-IR spectrum was collected at 150 °C with an accumulation of 64 scans at a 4 cm^{-1} resolution (called reference spectrum). The temperature was reduced to around 50 °C and pyridine vapor was introduced until saturation. Subsequently, the thermal desorption of pyridine took place at temperatures of 150 °C, for 2 h, under vacuum and a spectrum was collected after this step. The density of BAS and LAS was measured by integrating the areas of the bands that are characteristic of these species, respectively the ones at 1545 cm^{-1} (using the molar coefficient ε_{BAS}

Published in : Chemical Engineering Journal (2025), vol. 523
DOI: 10.1016/j.cej.2025.167966
Status : Postprint (Author's version)

= 1.67 cm/μmol) and 1455 cm^{-1} (using ε_{LAS} = 2.22 cm/μmol) as described in literature reports[33],[34]. To calculate the amount of acid sites the following formulas were used:

$$d_{BAS} = \frac{A \bullet S}{\varepsilon_{BAS} \bullet m} \quad (10)$$

$$d_{LAS} = \frac{A \bullet S}{\varepsilon_{LAS} \bullet m} \quad (11)$$

where d_{BAS} and d_{LAS} are the density of Brønsted and Lewis acid sites, respectively (μmol/g), A is the integrated area of the adequate band (cm^{-1}), S is the surface of the pellet (cm^2), ε_{BAS} and ε_{LAS} are the molar coefficients of BAS and LAS, respectively (cm/μmol), and m is the weight of the pellet (g).

The determination of the contribution of external and internal SiOH in the SiOH band was estimated by applying a peak deconvolution in the 3770–3690 cm^{-1} region using OMNIC software. Two SiOH groups were considered for the SiOH band, namely external SiOH (in the range 3742–3740 cm^{-1}) and internal SiOH (in the range 3735–3731 cm^{-1}). After a baseline correction of the spectra in the zone of interest, a deconvolution procedure using Voigt peaks fitting was applied with ±2 cm^{-1} of freedom on the peaks position. An example is shown in Fig. S5.

2.4.3. SCANNING ELECTRON MICROSCOPY (SEM)

To show the size of the particles of the zeolites and their aggregates, SEM images were taken. SEM was performed using a microscope JEOL JSM-6010LV at a voltage of 15 or 20 kV, after the samples were attached to a carbon tape and coated with a layer of Pd/Au of a ratio of 60/40 in order to ensure conductivity. *2.4.4. N_2 physisorption*

To estimate the surface area and the pore volume of the zeolites, N_2 physisorption was performed using the Tristar II 3020 equipment from Micrometrics. The samples were pretreated at 350 °C overnight before the measurement. The measurement was conducted by varying the relative pressure of nitrogen (p/p_0) at 77 K. To calculate the micropore volume, the Harkins and Jura t-plot method was used (Table S2).

2.4.5. THERMOGRAVIMETRIC ANALYSIS (TGA)

The water and coke contents of the used catalysts were measured using a Mettler Toledo TGA/DSC 3+. A treatment protocol with varying gas flows and temperatures was used as reported in the literature [35]. Firstly, a ramp of temperature at 10 °C/min up to 200 °C under N_2 resulted in weight loss of the catalyst due to the water desorption. Consequently, further increase of temperature up to 600 °C (5 °C/min) under N_2 indicated the loss of weight due to the loss of soft coke. At the final step, the gas used was switched to O_2 and the temperature stayed at 600 °C for 30 min. However, due to lack of knowledge of the exact coke composition, all coke content is calculated as an average between some products indicated by literature as described later in paragraph 3.2.

Published in : Chemical Engineering Journal (2025), vol. 523
DOI: 10.1016/j.cej.2025.167966
Status : Postprint (Author's version)

3. Results and discussion

3.1. COMPARISON BETWEEN ZNZRO$_X$ AS CATALYST FOR CTM AND TANDEM CONFIGURATION OF ZNZRO$_X$ + ZEOLITES FOR THE ONE-STEP CO_2 TO HYDROCARBONS

At first, $ZnZrO_x$ was tested in CTM at 40 bar with varying temperatures from 260 to 360 °C (Fig. 1a). With increased temperatures, the conversion of CO_2 was increased leading to higher STY of MeOH and CO, with the highest STY of MeOH being at 340 °C (8.5 molC/g_{cat}/h). Above this temperature (at 360 °C), RWGS reaction becomes more dominant leading to more CO production (Fig. 1 a) [36]. When $ZnZrO_x$ was coupled with a beta zeolite, the methanol pathway was ensured because it was proven that the CO does not get converted (STY values of CO show only a slight decrease when zeolite is added, in all temperatures tested, and this difference decreases with increasing T, and at the same time the system errors are reduced due to the higher amounts measured, reaching a 9 % of CO decrease in 340 °C when zeolite is added, which is considered insignificant), in contrast to MeOH which gets almost fully reacted as shown in Fig. 1 b. To have a better comparable system, the experimental set for CTM presented in Fig. 1b was conducted keeping the exact same layer of $ZnZrO_x$, in terms of mass and volume, and the same feed flow, as in the case of Fig. 1a, but now with the addition of a beta zeolite layer. This means that the GHSV in the case of Fig. 1a was double (17,000 Nml.g_{cat}^{-1}.h^{-1}) due to the lower amount of total catalyst present. For comparison in Fig. 1b, the values of STYs for sole CTM were divided by half, and the comparable calculated results were presented. Another way to do this would be to calculate all products formed in the tandem on a $ZnZrO_x$ basis (which would mean doubling the obtained STYs in Fig. 1b to plot against the Fig. 1a ones). The conversion of CO_2 was slightly increased when a zeolite bed was added, especially at high temperatures, proving the presence of the catalytic coupling (and its potential), meaning that the product of the first part of the reaction (MeOH) gets further converted leading to enhance the conversion of the initial feed of gases (CO_2 and H_2). This can also be noticed from the Space Time Conversion (STX, mol CO_2 converted/h/kg_{cat}) which also increases with the addition of the zeolite. With the temperature increasing, both the conversion and the STYs of the products increase. The produced hydrocarbons are mainly aliphatics (more detailed product distribution and selectivities are discussed in Section 3.2) and the highest STY of paraffins (2.8 molC/kg_{cat}/h) was reached at 340 °C. However, given that we are aiming to keep the selectivity to CO at a lower level, 300 °C was chosen as an adequate temperature for further catalytic screening.

Published in : Chemical Engineering Journal (2025), vol. 523
DOI: 10.1016/j.cej.2025.167966
Status : Postprint (Author's version)

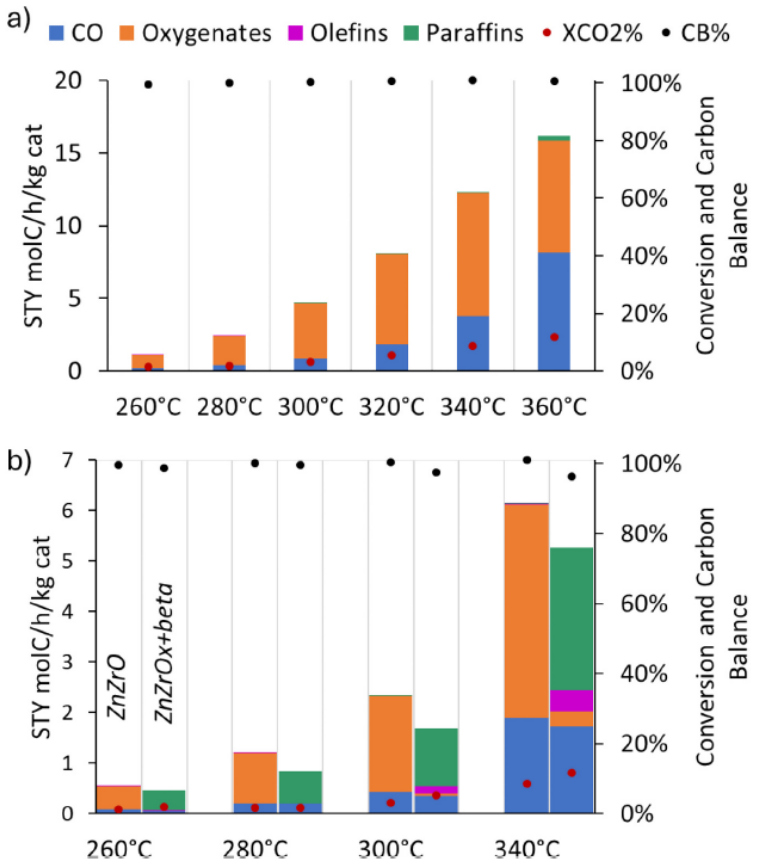

Fig. 1. Catalytic performance on different temperatures of a) pure $ZnZrO_x$: 150 mg, 42.5 Nml.min equaling a GHSV = 17,000 Nml.g_{cat}^{-1}.h^{-1} P = 40 bar and b) $ZnZrO_x$ + Beta Si/Al = 15 (dual bed configuration with $ZnZrO_x$:Zeolite = 1:1): 300 mg, 42.5 Nml.min equalling a, GHSV = 8500 Nml.g_{cat}^{-1}.h^{-1}, P = 40 bar. For comparing in 1b, the 1a data is recalculated by halving it, based on the fact that the $ZnZrO_x$ + beta STYs are divided in the denominator by double the total weight of catalyst. Oxygenates = mainly methanol (100 % MeOH 260–300 °C, 80 % MeOH at 340 °C), Olefins = mainly C2-C3 alkenes, Paraffins = mainly C4-C6 alkanes.

3.2. CATALYTIC EFFECT OF THE BED CONFIGURATION

3.2.1. BED CONFIGURATION AND ACIDITY

To elucidate the effect of the bed configuration, two types of proximity levels were studied, i.e. mixed bed and dual bed (as defined in the introduction), for a range of zeolites (beta and MFI topologies) owning different Si/Al ratios (Fig. 2). Before discussing in detail the catalytic results of the tandem system it is worth mentioning that during blank tests (no catalyst present in the reactor) at 40 bar of pressure and 300 °C, no reaction is observed and only the feed gases are detected at the exit of the system. It is shown that in every case, the dual bed configuration is beneficial for obtaining higher STYs of paraffins compared to the mixed bed configuration. However, in some cases, such as for ZSM-5 40 and beta 20 zeolites, this effect is minimal: these zeolites showed a high STY of paraffins in dual bed configuration (1.4 and 1.3 molC.kg_{cat}^{-1}.h^{-1}, respectively) but also in mixed bed configuration (0.9 and 1 molC.kg_{cat}^{-1}. h^{-1}, respectively). Surprisingly, beta 15, that showed a poor STY of paraffins in the mixed bed configuration (0.3 molC.kg_{cat}^{-1}.h^{-1}), was the most active in producing paraffins in the dual bed configuration (1.7 molC.kg_{cat}^{-1}.h^{-1}). As presented in Fig. 2b, in all cases the main products are C4 (n-butane and isobutane), and beta with Si/Al 15 shows the highest STY of these products, with the

Published in : Chemical Engineering Journal (2025), vol. 523
DOI: 10.1016/j.cej.2025.167966
Status : Postprint (Author's version)

exception of ZSM-5 which shows more C5+ hydrocarbon production. Exact product distributions are presented in Table S3.

The particle sizes of the beta zeolites used were measured and some minor variations were found as shown in Fig. S6. In the aim to better understand the different catalytic behavior of the studied zeolites, we calculated and compared their surface acid density (BAS and LAS) using pyridine probe FT-IR spectroscopy (Fig. S7). Table 1 reports the obtained densities for both BAS and LAS in comparison to the commercial supplier Si/Al ratios. The total acid site density is expected to decrease with higher Si/Al ratios, however, this trend is not always respected since non-acidic Al species (and also Al agglomerates) can be present in different proportions[33],[37]. For example, beta 12.5 exhibits lower acid sites density than beta 15 and beta 20 zeolites. As for the methanol conversion capacity, the zeolite with the highest BAS density (beta 15) showed the highest STY of hydrocarbons, but only in the dual bed configuration (Fig. 2).

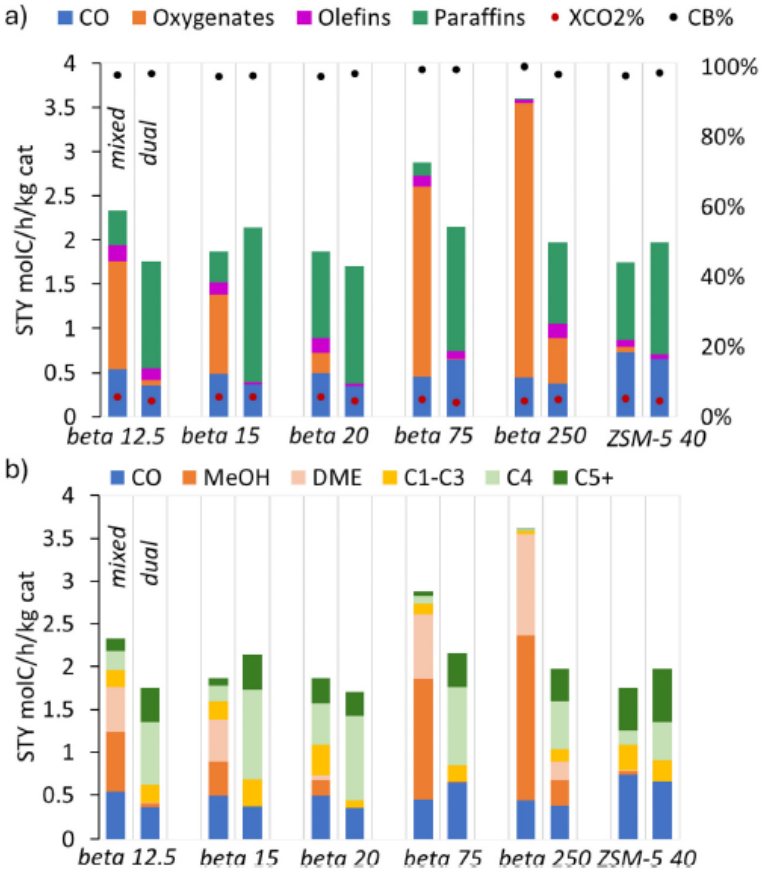

Fig. 2. a) Catalytic performance of different zeolites (zeolites beta with different Si/Al ratios and ZSM-5) in 2 proximities (mixed and dual bed configuration) given in STY (molC.$kg_{cat}^{-1}.h^{-1}$), conversion of CO_2 and Carbon Balance and b) more detailed products distribution given in STY (molC.$kg_{cat}^{-1}.h^{-1}$) showing CO, MeOH, and DME as well as the hydrocarbons grouped in chain length ranges. $ZnZrO_x$:Zeolite = 1:1, T = 300 °C, P = 40 bar, GHSV = 8500 Nml.$g_{cat}^{-1}.h^{-1}$.

Published in : Chemical Engineering Journal (2025), vol. 523
DOI: 10.1016/j.cej.2025.167966
Status : Postprint (Author's version)

Table 1
Densities of Brønsted Acid Sites (BAS) and Lewis Acid Sites (LAS) based on FT-IR measurements for zeolites with different Si/Al ratios.

Sample	Si/Al	BAS (μmol/g)	LAS (μmol/g)	Total acidity (μmol/g)	BAS/LAS
beta12.5	12.5	201	114	315	0.9
beta 15	15	348	121	469	2.9
beta 20	20	281	95	376	3.0
ZSM-5 40	40	163	37	200	4.4
beta 75	75	64	8	72	8.0
beta 250	250	25	4	29	6.2

Note: The coefficient of variation (100*SD/Mean) on the BAS and LAS values (for 3 measurements) was estimated in the range of 4 to 11 %.

A correlation was attempted between the BAS density and the STY of hydrocarbons for both tested configurations (Fig. S8). As it has been shown in literature, BAS are mainly responsible for the dehydration of methanol to the essential intermediates for MTH [12],[38]. This is confirmed by Fig. S8a, which shows that in mixed bed configuration, the increase of BAS leads to a decrease in STY of oxygenates, meaning that those species are further converted in the presence of more Brønsted acid sites. This trend is reported for the mixed bed configuration because in that configuration the amount of oxygenates is significant (as shown in Fig. 2) allowing this interpretation. As for the dual bed, Fig. S8b shows that in this configuration, zeolites with higher BAS amount can result in higher paraffins STY. Dual bed was chosen here to represent this effect due to the higher amounts of paraffins produced (Fig. 2) and the lack of other parameters present that could affect the result, such as variability added from mixing. It is worth noting that the results are presented in terms of total weight of catalyst but to fully understand the catalytic potential of the zeolites, the STYs are presented in Fig. S9 in terms of mols of Al with the hypothesis that BAS are mainly responsible for the activity. As shown, beta 75 and beta 250 have a very high activity considering their Al content which could possibly mean that their performance could be enhanced in a differing experimental configuration. In addition the comparison of the catalytic behavior of zeolites is done under specific conditions, with the focus on determining differences due to the bed configurations, but different conditions could potentially enhance or reduce the activity of some of the zeolites.

The analysis of the evolution of the OH zone during pyridine adsorption and desorption experiments (shown in Fig. 3b) was applying a subtraction of the spectra: the spectrum after activation (reference spectrum shown in Fig. 3a) minus the spectrum obtained after pyridine desorption at 150 °C. By applying this subtraction order, we will be able to point out (as the positive remaining bands) the OH species that were consumed by pyridine adsorption. Herein, the different OH species and their contribution in the acidity (interacting with pyridine) can be estimated by integrating the peaks corresponding to each.

Published in : Chemical Engineering Journal (2025), vol. 523
DOI: 10.1016/j.cej.2025.167966
Status : Postprint (Author's version)

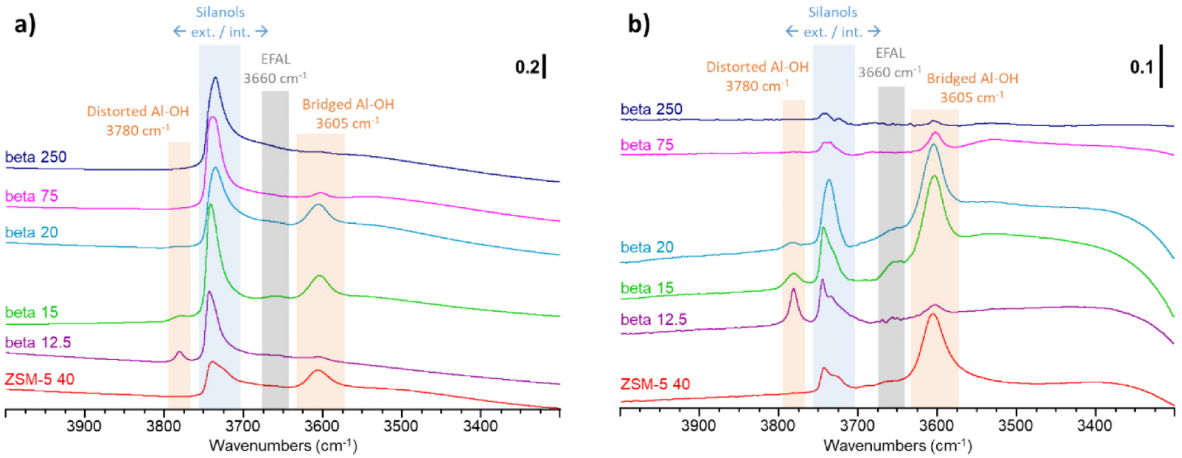

Fig. 3. FT-IR spectra for the studied zeolites showing the OH stretching zone from 4000 to 3300 cm^{-1}, where different surface hydroxyl species can be observed (Terminal Al-OH, Internal and external silanols, framework Al-OH, and EFAl: extra-framework Al phase). Figure (a) shows the OH stretching zone of the reference samples (after activation and before the addition of pyridine) and (b) reports the OH stretching zone of the subtraction spectra obtained from pyridine adsorption and desorption at 150 °C. Each spectrum in (b) is obtained by doing the spectrum of a sample after desorption at 150 °C minus the reference spectrum of that same sample before the addition of pyridine. This illustration allow to visualize and compare the OH groups in interaction with pyridine (the ones responsible of BAS) on each sample.

Besides the amount of BAS and LAS, the acid sites location and nature have been found in previous studies to affect and, even in some cases, to be essential for the selectivity and the activity of the zeolite in a MTG reaction [39],[40]. The nature of the surface hydroxyl species for the studied zeolites was also investigated using FT-IR spectroscopy analysis of the OH stretching vibration zone. Four main surface hydroxyl species could be evidenced in different contributions in the studied zeolites, namely, distorted Al-OH at 3780 cm^{-1}, silanol groups (both external ≈ 3740 cm^{-1} and internal ≈ 3725 cm^{-1}), extra-framework Al phase (EFAl) at around 3660 cm^{-1}, and bridged Al-OH at 3605 cm^{-1} (Fig. 3a) [41]. Pyridine adsorption and desorption at 150 ˚C was performed to depict the acidic OH groups that are prone to retain pyridine at 150 ˚C (Fig. 3b). The two zeolites that show the smallest influence by altering the bed configuration from mixed to dual are Beta 20 and ZSM-5 40. Even though the topologies and Si/Al ratios are different, these two zeolites show the highest ratio of acidic bridged Al-OH to acidic silanols.

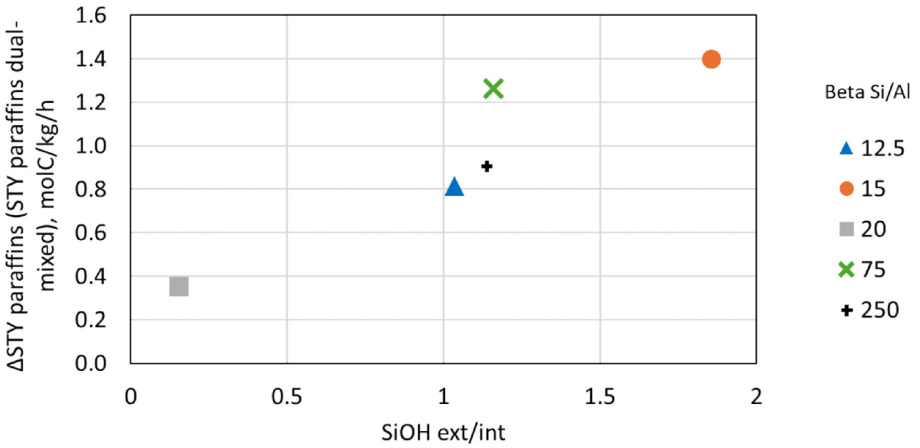

Fig. 4. Correlation between the ratio of external SiOH to internal SiOH present in zeolite beta with different Si/Al, with the ΔSTY paraffins (STY paraffins in dual bed configuration – STY paraffins in mixed bed configuration). The area of the silanol groups is from deconvoluting the relevant IR peaks: external silanol groups ≈ 3740 cm^{-1} and internal silanol groups ≈ 3725 cm^{-1}.

Published in : Chemical Engineering Journal (2025), vol. 523
DOI: 10.1016/j.cej.2025.167966
Status : Postprint (Author's version)

However, Beta 15, which also possesses a high ratio, presents large variations with the different bed configurations. In addition, correlations between IR-based signals and the difference between the STY of paraffins in dual and mixed bed configuration (ΔSTY paraffins) were attempted. These correlations between e.g. EFAl, terminal Al-OH, Framework Al-OH, external and internal SiOH and ΔSTY of paraffins for beta zeolites were plotted, yet without success in giving a clear trend to help in understanding the difference in the behavior or paraffin production in mixed and dual bed. Amongst the different hydroxyl species measured, the ratio of external silanols to internal ones was the only one found to show some correlation to the ΔSTY paraffins, as shown in Fig. 4. This could indicate that a beta zeolite with higher ext./ int SiOH ratio benefits more from a dual bed configuration rather than one with a lower ratio, for which the bed configuration effect is less dominant. The role of silanols has been shown in literature where it is indicated that external silanols of zeolites (crystalline materials) have acidic nature either weaker or moderate and can improve the performance of the catalyst in certain reactions [42],[43]. This trend is mostly present when comparing Beta 15 and Beta 20 which have very different catalytic behavior when altering the proximity even though they have a small Si/Al difference. It should be stated, however, that the choice of the optimum bed configuration is dependent on several parameters and not only the topology and the nature and location of the acid sites.

It has been shown in literature that the interaction of alkanes with the active sites of the zeolites happens through van der Waals forces or induced dipole interactions with oxygens of the framework of the zeolite [44]. By increasing the void size of the zeolite, however, these interactions become weaker, indicating the importance of the void and consequently pore size of the zeolite for these reactions [44]. When talking about one specific topology (e.g., beta), the void size is theoretically the same, even though in reality we expect minor differences due to the different synthesis and the different Si/Al ratios. One way that could potentially explain further the drastic differences due to the bed configuration, is the altering of the void 'space' that is left for the molecules to interact. In mixed bed configuration, MeOH produced from the $ZnZrO_x$ (throughout the whole bed length) can directly occupy the pore space in the neighboring zeolite, likely leading to hydrocarbons formation and chain growth reactions inside the zeolites. This will allow only specific-sized hydrocarbons to escape (simulation studies have been performed on whether molecules e.g. benzene can diffuse the original cage or not [45]). However, in dual bed configuration, we could assume that MeOH molecules will occupy the zeolite particles of the top of the zeolite bed (the first part of the zeolite right after the $ZnZrO_x$ layer), while formed hydrocarbons can occupy the zeolite particles underneath. In that way, more surface reactions can take place (not only inside the pores of the zeolites), enhancing the selectivity to longer chain hydrocarbons. This could, although this is hypothetical, explain why zeolites with highly abundant acidic external silanols (≈ 3740 cm^{-1}), in comparison to the internal ones, were found to have the most intense improvements when used in dual bed. In that way having hydrocarbons reacting both inside the zeolite pores and on the outside opens many possibilities in understanding and optimizing the materials to get better selectivity results in the future. In addition, the fact that longer chain hydrocarbons are not forced to stay in the pores due to their inability to escape (because of size limitations that play the most important role in mixed bed), but could also react on the surface of the zeolite can be a reason for the general trend of slower deactivation in the dual bed configuration experiments (Fig. S10, with the exception of beta Si/Al = 250 which shows a fast deactivation pattern in both bed configurations perhaps due to the very low amount of BAS (Table

Published in : Chemical Engineering Journal (2025), vol. 523
DOI: 10.1016/j.cej.2025.167966
Status : Postprint (Author's version)

1) which are occupied by methanol, inhibiting further reactions [46]), as pores maybe do not get clogged as fast from the heavier compounds [40]. This can be also indicated by studies that show that internal silanols can be detrimental for faster deactivation of the zeolite, such as in the case of ZSM-5 for the MTH reaction [42].

Zhang et al., studied the influence of BAS (amount and density) in the MTG reaction over Beta zeolites and found that by altering the density, different mechanistic pathways can be enhanced or inhibited [46]. According to the study, decreasing the BAS density favors the olefin interconversion reactions (methylation and cracking) while suppressing the hydrogen transfer one. The same effect was observed when the methanol concentration was increased as it is the reactant of the methanol induced hydrogen transfer reaction. When BAS density is high (crowded active sites), each active site encounters less methanol which then leads to lower conversions of methanol needed in the hydrogen transfer reactions and consequently leading to less alkane and aromatic formation. They found that the main reason for deactivation in this system is mainly the polycyclic aromatics and secondly the long-chain alkanes. Higher BAS densities decrease the alkanes but increase the polycyclic aromatics which then lead to faster deactivation [46]. Interestingly, in the present work this is not confirmed directly as seen in Fig. S10, where Beta 15 and 20 (highest BAS, Table 1) show the most stable behavior in dual bed configuration. In this case, the presence of H_2 and CO_2 in large amounts has a major impact on the system, as well as the bed configuration as described earlier. More specifically, altering the bed configuration, alters the methanol concentration available for each active site resulting to different catalytic performances under given conditions. This confirms the importance of Al-OH species to the mechanistic pathways followed for each proximity level.

Investigating the TOS catalytic results (Fig. S10), some interesting observations are made. As expected, when Beta 20 is used for the MTH part of the tandem reaction, the deactivation (increase of oxygenates and at the same time decrease of paraffins, as measured in the products) becomes fast compared to the rest of the zeolites. This can be explained by the highest overall amount of internal silanols, present in Beta 20, which have been found to be responsible for enabling coke formation [42],[47]. Interestingly this only applies to the mixed bed configuration. It is shown that when changing the bed configuration to dual, not only slightly higher STYs of paraffins are achieved (comparing the 1st hour performance of each experiment), but also the deactivation becomes much slower, reaching almost stable values even after 8 h of experiment. The opposite trend is noticed for the Beta 250. When in mixed bed configuration the system is stable but, in contrast, when in dual bed, the deactivation is very fast. However, it must be underlined that in that case, Beta 250 in mixed bed, is not active towards hydrocarbons but only towards DME. Beta 12.5 appears to deactivate as well but at a slow rate which is consistent in both bed configurations. The rest of the zeolites show an almost stable behavior for both proximities.

3.2.2. BED CONFIGURATION AND GHSV

Investigating further the factors that contribute to altering the reaction in the different bed configurations, a study on GHSVs was conducted as a way to show whether altering the residence time can affect the behavior due to different proximities. Beta 15 was chosen for further investigation because it shows the best performance in terms of STYs of paraffins and has a relatively stable performance during the experimental time. Also, for the dual tandem systems $ZnZrO_x$ + beta 15 and

Published in : Chemical Engineering Journal (2025), vol. 523
DOI: 10.1016/j.cej.2025.167966
Status : Postprint (Author's version)

$ZnZrO_x$ + beta 20, reproducibility was tested (Fig. S11), showing that the results are sufficiently reproducible throughout the duration of the experimental work presented here. Note that theoretically, GHSV is Nml (normal milliliter) of gas flowing per time unit, divided by ml of catalyst bed volume. Yet, since densities can vary, an expression more functional at the lab scale is $Nml.g_{cat}^{-1}.h^{-1}$ Fig. 5a shows that the conversion of the reaction is negatively affected by increasing the GHSV (logically, as the residence time lowers), while the opposite trend was observed for the STY which showed the highest overall amount of paraffins (1.5 molC. $kg_{cat}^{-1}.h^{-1}$) produced at GHSV = 21,000 $Nml.g_{cat}^{-1}.h^{-1}$. At higher GHSV, the STY of i-C4 increased to almost 1 $molC.kg_{cat}^{-1}.h^{-1}$ but the selectivity of all paraffinic products dropped and the selectivity of i-C4 remained stable showing the formation of more by-products as well. At the same time, it was observed that in all tests MeOH was only fully converted when a dual bed configuration was applied. On the other hand, when a physically mixed bed configuration was used, oxygenates (MeOH and DME) are still present, even more as dominant products. In Fig. 5b the exact product distribution is presented. It was noticed that in the mixed bed configuration MeOH is partially converted to DME whereas in the dual one, the main product is isobutane. An increasing GHSV has a negative effect on the mixed bed experiment throughout the whole range of increase whereas it has a positive effect for the dual bed experiment for the STYs of desired products (Fig. 6). The highest selectivity of i-C4 amongst products (39 %) was obtained in dual bed configuration at GHSV = 8500 $Nml.g_{cat}^{-1}.h^{-1}$. Moreover, the STY of C5+ products almost doubled (up to 0.5 $molC.kg_{cat}^{-1}.h^{-1}$, when GHSV increased to 21,000 $Nml.g_{cat}^{-1}.h^{-1}$. Interestingly, the selectivity of paraffins slightly decreased when GHSV increased from 8500 to 21,000 $Nml.g_{cat}^{-1}.h^{-1}$, which can be explained by the enhanced STYs of CO and C1-C3 products.

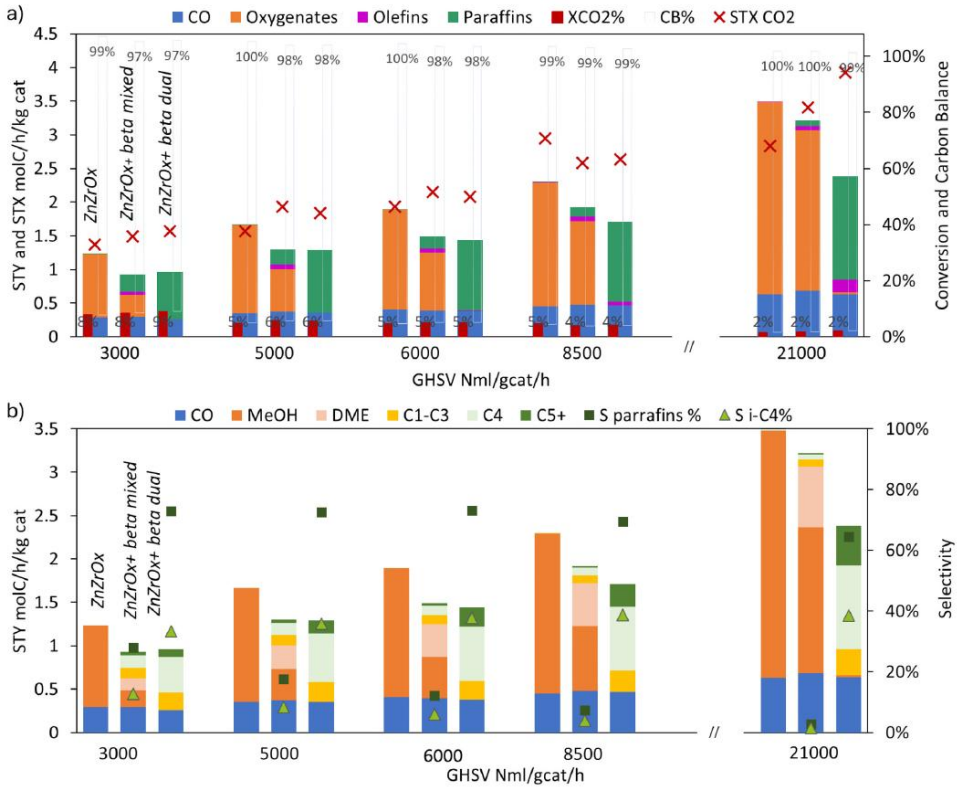

Fig. 5. Effect of GHSV on reactions with $ZnZrO_x$ only and on tandem systems with different bed configuration of $ZnZrO_x$ and beta zeolite (Si/Al = 15) at 300 °C and 40 bar. a) STY of the products and CO_2 conversion (both % and in STX) and carbon balance, b) exact product distribution and selectivity of main products. Selectivity of paraffins = total paraffins present in the products (including isobutane), selectivity of isobutane = isobutane selectivity over all products present.

Published in : Chemical Engineering Journal (2025), vol. 523
DOI: 10.1016/j.cej.2025.167966
Status : Postprint (Author's version)

It needs to be underlined that, as presented in Fig. 6, the different bed configurations give very different trends. For the mixed catalysts, the trend of STYs and selectivities follows the CO_2 conversion trend while in dual bed configuration, this trend is only followed at higher GHSVs and only for the selectivities and not for the actual STYs.Trying to relate the observed differences between the bed configurations and the GHSV, it was assumed that the partial pressure of the methanol produced by the oxide (first reaction step) works as the input for the zeolite (second reaction step) for the dual bed configuration. The theoretical partial pressure at the outlet of the $ZnZrO_x$ layer was calculated based on experimental data in which the impact of the GHSV was studied in the presence of a single catalyst layer, namely the $ZnZrO_x$ layer (testing the pure oxide as seen in the first bars of Fig. 5). Then the zeolite was added, and the same experimental procedure was used and the partial pressure of the interesting products was then calculated at the output of the tandem system. Fig. 7 demonstrates how the theoretical partial pressure of MeOH as the feed to the zeolite correlates with or affects the partial pressure of the final products after the zeolite bed. In normal reaction conditions, in a dual bed configuration, MeOH is not observed as a product because it is getting directly and fully converted further. Fig. 7 shows that as the partial pressure of MeOH increased, the final partial pressure of i-C4 also does. A negative effect was observed for the production of olefins. The gasolinic hydrocarbons (C5+) were only slightly influenced by the increase of the partial pressure of the intermediate product of the tandem system. It is shown that even a very small partial pressure of methanol (0.1 kPa, utmost left point) is enough to initiate the production of hydrocarbons in the case of dual bed. This opens the discussion for a further possibility to control the methanol partial pressure of the feed to the zeolite when the catalytic layers are separated further, offering tools for enhancement of such tandem catalysis.

3.2.3. BED CONFIGURATION AND COKING

In an effort to further investigate how the different proximity affects the reaction and the catalysts, TGA was used to measure the coking of the catalysts after reaction as presented in Fig. 8a. The TGA method used allowed the differentiation between the weight loss due to water present in the used catalyst and the removal of the coke. Assumingly, at the first step of the method (increasing the temperature under N_2 atmosphere), the loss of the mass is being attributed to water in the catalyst and more specifically inside the pores of the zeolite and this is expected to be completed by 200 °C. With further increase of the temperature, and at the final step, adding O_2, the weight reduction derives from the burning of the cokes. For the identification of components illustrated in Fig. 8b, coke components are calculated based on relevant studies for MTG reaction [48],[49]. In the work of H. Schulz, the deactivation pattern of H- Beta was shown and the coke H/C ratio was found to be 0.8. However the MTG was conducted at 475 °C in that case whereas in the recent work the working temperature is 300 °C [48]. Regeneration of H-ZSM-5 after MTG was studied in the same work at a emperature of 290 °C, showing a coke H/C ratio of 1.64 [48]. In order to help with the calculations, 2 molecules were assumed as main coking products with following H/C ratios, $C_{10}H_8$ and $C_{10}H_{16.4}$.

Published in : Chemical Engineering Journal (2025), vol. 523
DOI: 10.1016/j.cej.2025.167966
Status : Postprint (Author's version)

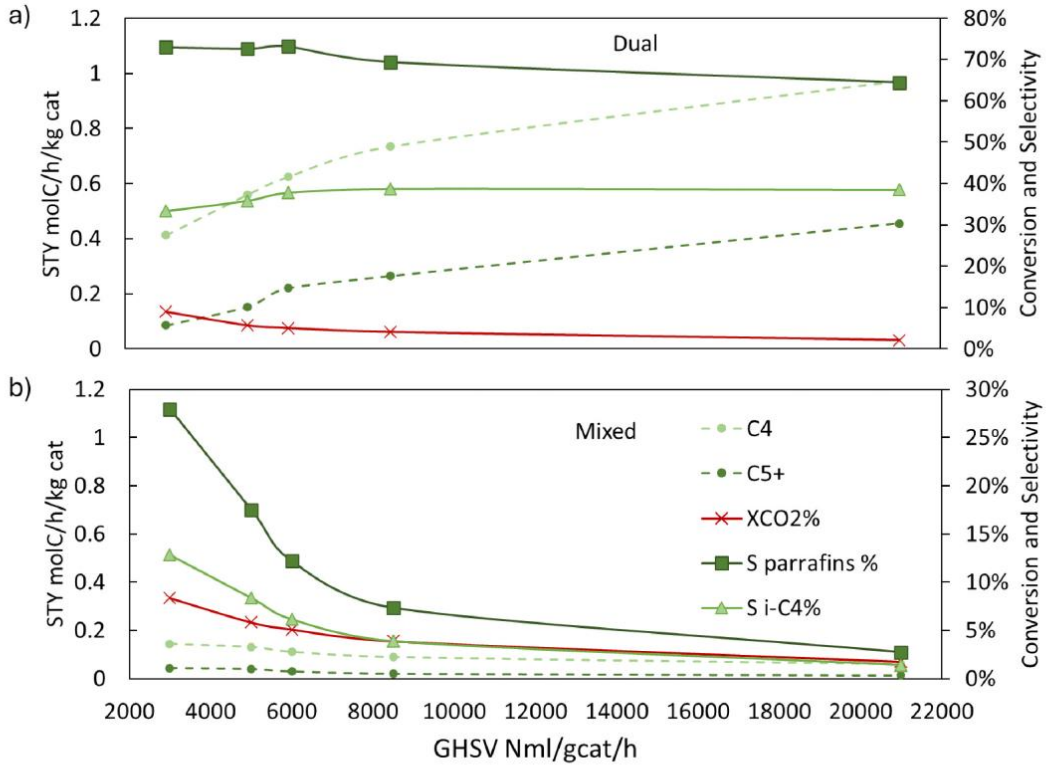

Fig. 6. Effect of GHSV on the tandem system of $ZnZrO_x$ and beta zeolite (Si/Al = 15) at 300 °C and 40 bar. a) STY of C4 (all C4 paraffins including i-C4) and C5+, CO_2 conversion and selectivities of paraffins and isobutane in dual bed configuration, b) STY of C4 (all C4 paraffins including i-C4) and C5+, CO_2 conversion and selectivities of paraffins and isobutane in mixed bed configuration. Selectivity of paraffins = total paraffins present in the products (including isobutane), selectivity of isobutane = isobutane selectivity over all products present. Note the different ranges of the righthand y-axis.

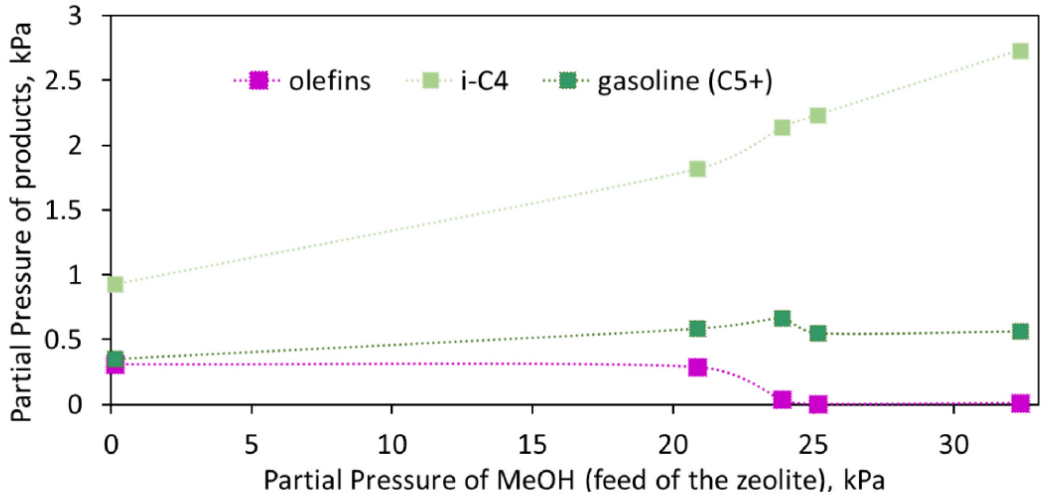

Fig. 7. Effect of theoretical partial pressure of methanol as feed (CO_2 to methanol catalyst) to the zeolite part (MTH) of the tandem system ($ZnZrO_x$ + Beta Si/Al = 15) in a dual bed configuration. The partial pressure of methanol was calculated theoretically from pure $ZnZrO_x$ experimental data conducted at different GHSV (Fig. 5). The partial pressures of the products have been calculated at the output of the reactor after online GC measurements. The connecting dashed lines are added only as a guide to the eye.

Published in : Chemical Engineering Journal (2025), vol. 523
DOI: 10.1016/j.cej.2025.167966
Status : Postprint (Author's version)

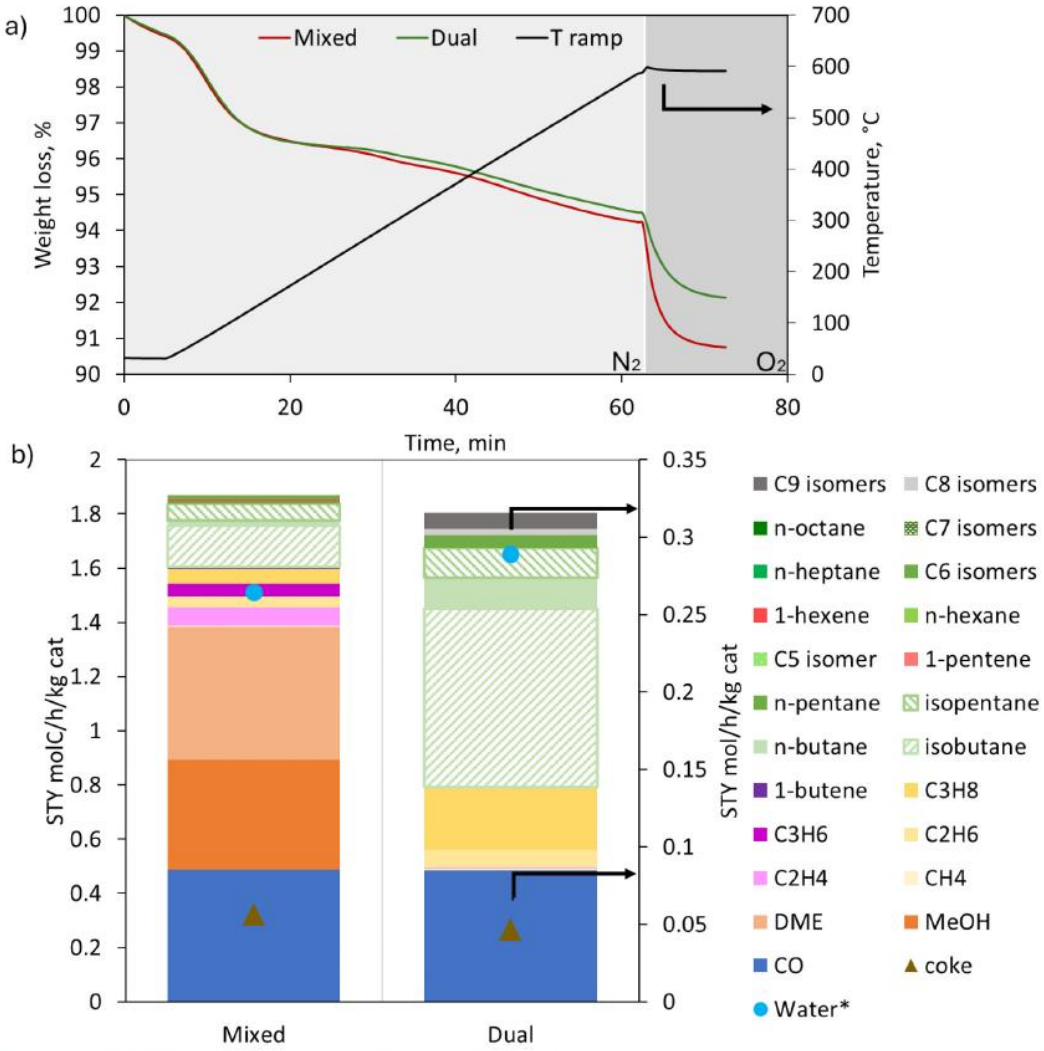

Fig. 8. Coke analysis and product details of the catalytic performance of $ZnZrO_x$ and Beta (Si/Al = 15) in mixed and dual bed configuration. (a) TGA of catalysts collected post reaction of mixed and dual bed configurations after 8 h of experiment with the ramp and gases in the background (b) STY of products and product distribution. Conditions: $T = 300$ °C, $P = 40$ °C, GHSV = 8500 $Nml.g_{cat}^{-1}.h^{-1}$. All products are measured online by the GC except for coke and water* which refers to the catalyst content post- reaction from TGA and are calculated and corrected based on the weight of the catalyst and the duration of the experiment. *water is added to the picture for the sake of completion and is calculated (not measured) as described.

Even though those 2 products are not realistic coke compounds, they are used theoretically for the calculation of a hypothetical molar mass of coke compounds. It should be underlined that many products (especially aromatics) formed in the cavities of the zeolite lead to coke formation but Beta, having specific cavities' size, can allow some of them to further diffuse in the channels (products such as methylated benzenes) [48]. As shown in Fig. 8, the amount of these components measured from the TGA weight loss, is not high which agrees with the slow deactivation observed and discussed later and could be due to the presence of high pressure H_2 which has been proved to improve the lifetime of the materials used for MTO [50]. Even in small amounts, there is a trend that shows that dual bed configuration results in higher amounts of water compared to the mixed bed, however the coke amount appears slightly lower for the case of dual bed, which can be expected due to the discussion above on the pores clogging with heavier compounds.

Published in : Chemical Engineering Journal (2025), vol. 523
DOI: 10.1016/j.cej.2025.167966
Status : Postprint (Author's version)

3.2.4. BED CONFIGURATION AND TIME ON STREAM STABILITY

The complexity of tandem catalysis leads to multiple challenges, and a major one is stability. Experiments were conducted for more than 30 has presented in Fig. 9 for mixed and dual beds. In both cases, CO_2 conversion and STY of CO are stable due to the lack of deactivation on the oxide part, which is the main responsible for these values. In addition, the STY of hydrocarbons (C2-C5+) is also relatively stable especially after 8 h of experiment. It is shown that even though in a dual bed configuration, the STY of fuel type alkanes (C4+) started as very high, it soon decreased while the STY of MeOH started to increase. However, the production of all products also seemed to stabilize after about 15 h. The same trend was observed for the mixed bed but in lower intensity. Interestingly, in dual bed configuration, the STY of isobutane and C5+ remain high even after 35 h on stream showing promising and stable behavior.

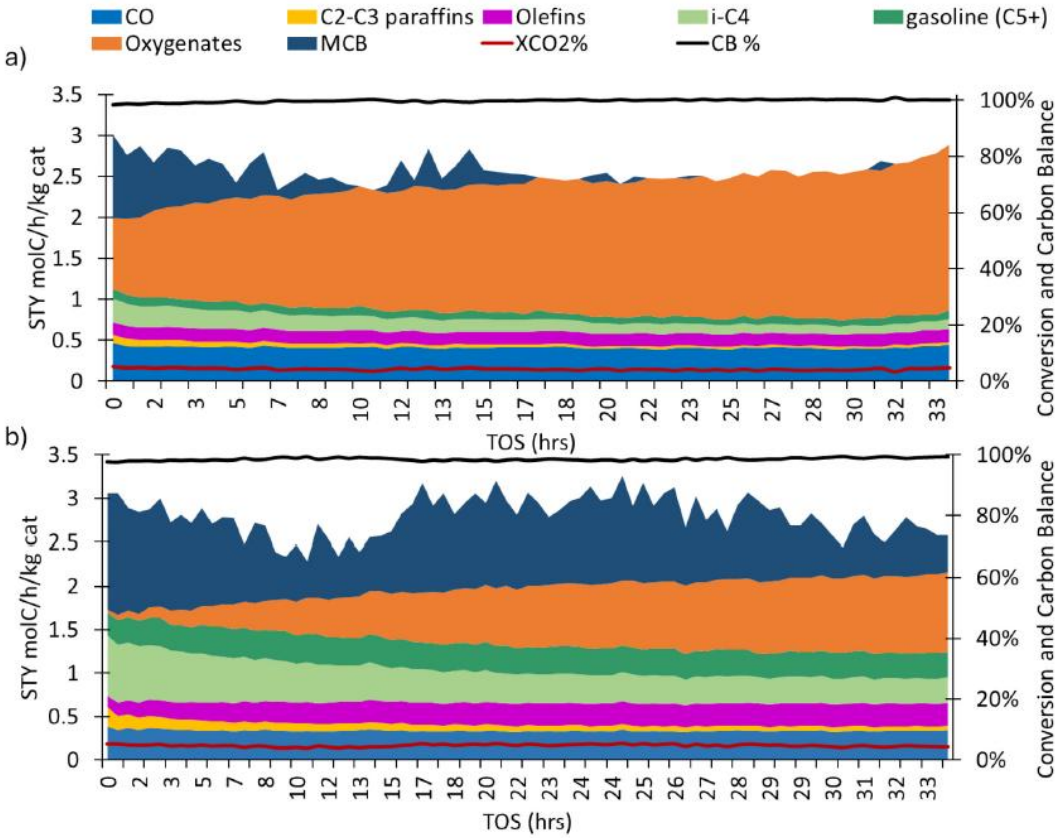

Fig. 9. Time on stream experimental data for 35 h of stability tests in (a) mixed bed configuration and (b) dual bed configuration. Conditions: T = 300 °C, P = 40 °C, GHSV = 8500 Nml.g_{cat}^{-1}.h^{-1}.

An important parameter that has been introduced in Fig. 9 is the "missing" carbon balance (MCB). This value indicates the amount of carbon that is not found in the output of the reaction (error of the CB) relatively to the carbon conversion. It is especially important here (and in this catalytic reaction overall) because even though the CB approached closely 100 %, the conversion was low enough (≈5 %) meaning that this error of the CB can be an important value when discussing STYs. Practically, having calculated the CO_2 in the input and output in terms of mols of carbon, and all the carbon mols deriving from the different products, there is always a small gap in the carbon mols balance (which is presented as the MCB) which as seen in Fig. 9 fluctuates with each point measured. This number can be affected

Published in : Chemical Engineering Journal (2025), vol. 523
DOI: 10.1016/j.cej.2025.167966
Status : Postprint (Author's version)

by many parameters. Some important parameters that affect the MCB can be the error of all equipment that was used for measurements but most significantly errors that occurred when measuring all components in the GC. It is obvious that this error potentially increases with the number of products that are measured, since there is a calibration error affecting each one of them. In addition, these errors include products that cannot be detected from the GC due to their properties that can be out of range for the method used for the GC injection (the GC run is approximately 1 h, while some longer hydrocarbons could potentially elute after that time). More so, products that appeared between known peaks of calibrated materials, were considered unknown but for calculation purposes they were assumed to be isomers with carbon number of the known range within which they appeared and were calculated accordingly. As presented in Fig. 9, higher MCB was connected to higher amounts of STY of targeted products, which is something potentially interesting. It could indicate the appearance of products of interest but out of the calibration range in the gas phase online analytical system (no collection of liquids is possible). Solutions to this problem could be challenging, it would imply for instance testing the tandem system in a more complex reactor in which phase separation is possible. This would allow more precise measurements of heavier compounds in a liquid phase. These type of systems could potentially provide more information on the role of water in the catalysis with these materials. It has been found that water is unavoidable and at the same time plays a significant role in the deactivation of both the oxide part and zeolite part of the tandem system [51]. In a different approach, i.e. MTG-focused studies, have shown that a slower deactivation occurs in the zeolite when water is present due to the molecules competing with coke precursor molecules in the adsorption on the acid sites of the catalyst but this behavior seems more dominant in lower temperatures and water concentrations (T > 450 °C, high water concentrations cause permanent deactivation on the zeolite) [52],[53].

4. Conclusions

In the present research work the combination of $ZnZrO_x$ and Beta zeolites was studied for the one-step methanol mediated hydrogenation reaction of CO_2 to fuels obtaining 36.4 % selectivity to isobutane. Dual bed configuration, where the 2 materials are positioned as layers one on top of the other in the reactor was found to benefit the production of paraffins. The combination of $ZnZrO_x$ and Beta zeolite 15 (Si/Al = 15) had the highest STY of paraffins amongst other Beta zeolites with different Si/Al ratios that were tested (1.75 $molC.kg_{cat}^{-1}.h^{-1}$). However, it was found that the different bed configuration might have a smaller effect in the product distribution for certain zeolites such as the reference ZSM-5 zeolite. FT-IR study on the different beta zeolites and the catalytic action were investigated showing a potential correlation between the ratio of external SiOH/internal SiOH and the bed configuration effect on the system, showing that higher ratio leads to higher ΔSTY of paraffins. It is proposed that void space and its filling with intermediate products is the reason for such behavior, as in mixed bed configuration MeOH is the dominant intermediate species throughout the whole zeolitic bed, whereas in dual bed, MeOH is only loaded in the first particles of the zeolite and longer chain hydrocarbons react with the rest of the bed perhaps more on the surface of the zeolitic particles. Further investigation altering this parameter on the same or different zeolites should be done in order to

Published in : Chemical Engineering Journal (2025), vol. 523
DOI: 10.1016/j.cej.2025.167966
Status : Postprint (Author's version)

obtain clear evidence for this hypothesis. Furthermore, the reaction conditions such as the GHSV and the temperature can also contribute to higher STYs of desired products. Interestingly it was found that at higher GHSV values, even though the conversion decreased significantly, the STY of desired products was increased leading however to an increase in undesired products such as CO as well. In addition, higher temperature benefits the STY of paraffins (reaching 2.8 molC.kg_{cat}^{-1}.h^{-1} at 340 °C) but simultaneously the STY of CO increases drastically. The materials were found stable for more than 30 h of experiment despite the initial (first 8 h) slow decrease in STY of targeted products (C4+) and increase in STY of intermediates such as oxygenates. The effect of water generated both in CTM and MTH is something that can play an important role in such catalytic systems but further investigation needs to be done in order to extract useful conclusions. While tandem systems don't show very high conversions and STYs, and there are still many influencing parameters them that need to be addressed (water, or the exact acid property-configuration relation), they can be interesting to selectively make a specific range of products (e.g. C4) and can show decent on-stream stability.

CREDIT AUTHORSHIP CONTRIBUTION STATEMENT

Foteini Lappa: Writing – review & editing, Writing – original draft, Visualization, Validation, Methodology, Investigation, Formal analysis, Data curation, Conceptualization. **Ibrahim Khalil:** Writing – review & editing, Writing – original draft, Visualization, Validation, Investigation, Formal analysis, Data curation. **Gregoire Léonard:** Writing – review & editing, Writing – original draft, Validation, Supervision, Resources, Project administration, Investigation, Funding acquisition. **Michiel Dusselier:** Writing – review & editing, Validation, Supervision, Software, Resources, Project administration, Methodology, Investigation, Funding acquisition, Conceptualization.

DECLARATION OF COMPETING INTEREST

The authors declare that they have no known competing financial interests or personal relationships that could have appeared to influence the work reported in this paper.

ACKNOWLEDGEMENTS

F.L., G.L. and M. D. acknowledge the main funding for this work: BE- HyFE project funded by the federal Energy Transition Fund by FPS Economy. I.K. acknowledges the Research Foundation Flanders (FWO Vlaanderen) for the Senior postdoctoral research grant (12A3M24N). M. D. acknowledges funding from KU Leuven grant C14/20/086.

APPENDIX A. SUPPLEMENTARY DATA

Supplementary data to this article can be found online at https://doi. org/10.1016/j.cej.2025.167966.

DATA AVAILABILITY

Data will be made available on request.

Published in : Chemical Engineering Journal (2025), vol. 523
DOI: 10.1016/j.cej.2025.167966
Status : Postprint (Author's version)

References

[1] F. Lappa, I. Khalil, A. Morales, G. Leonard, M. Dusselier, One Step Methanol- Mediated CO 2 Conversion to Gasoline: Comprehensive Review and Critical Outlook, Energy and Fuels 38 (2024) 18265–18291, https://doi.org/10.1021/acs. energyfuels.4c03013.

[2] M.S. Pr´evot, et al., An anthropocene-framed transdisciplinary dialog at the chemistry-energy nexus, Chem. Sci. 15 (24) (2024) 9054–9086, https://doi.org/ 10.1039/d4sc00099d.

[3] Intergovernmental Panel on Climate Change, Technology-specific cost and performance parameters, Clim. Chang. Mitig. (2015) 1329–1356, https://doi.org/ 10.1017/cbo9781107415416.025.

[4] S. Garg, Z. Xie, J.G. Chen, Tandem reactors and reactions for CO2 conversion 1 (February) (2024) 139–148, https://doi.org/10.1038/s44286-023-00020-2.

[5] W. Li, K. Wang, G. Zhan, J. Huang, Q. Li, Hydrogenation of CO2to dimethyl ether over tandem catalysts based on biotemplated hierarchical ZSM-5 and Pd/ZnO, ACS Sustain. Chem. Eng. 8 (37) (2020) 14058–14070, https://doi.org/10.1021/ acssuschemeng.0c04399.

[6] A. Boretti, Carbon dioxide hydrogenation for sustainable energy storage, Int. J. Hydrogen Energy 58 (February) (2024) 1386–1395, https://doi.org/10.1016/j. ijhydene.2024.01.199.

[7] F. Mahnaz, et al., Selective valorization of CO2 towards valuable hydrocarbons through methanol-mediated tandem catalysis, ChemCatChem 15 (17) (2023), https://doi.org/10.1002/cctc.202300402.

[8] A. Sajid, J. Devos, S. Robijns, T. Donckels, I. Khalil, M. Dusselier, Role of coupling and zeolite acidity in the methanol-mediated CO2 conversion to olefins over ZnZrOx-AEI zeolite tandem catalysis, J. Catal. 442 (December) (2025) 115927, https://doi.org/10.1016/j.jcat.2024.115927.

[9] T. Zhao, et al., Compound catalyst of ReMoSx@HSSZ-39 and SAPO-34 zeolites for high performance conversion of CO2 to C2-4 hydrocarbons, Chem. Eng. J. 497 (July) (2024), https://doi.org/10.1016/j.cej.2024.154448.

[10] A. Bakhtyari, M. Parhoudeh, M. Reza, Optimal conditions in converting methanol to dimethyl ether, methyl formate, and hydrogen utilizing a double membrane heat exchanger reactor, J. Nat. Gas Sci. Eng. 28 (2016) 31–45, https://doi.org/10.1016/ j.jngse.2015.11.028.

[11] A. Brunetti, M. Migliori, D. Cozza, E. Catizzone, G. Giordano, G. Barbieri, Methanol Conversion to Dimethyl Ether in Catalytic Zeolite Membrane Reactors, 2020, https://doi.org/10.1021/acssuschemeng.0c02557.

[12] H. Bahruji, R.D. Armstrong, J. Ruiz Esquius, W. Jones, M. Bowker, G.J. Hutchings, Hydrogenation of CO2 to dimethyl ether over brønsted acidic PdZn catalysts, Ind. Eng. Chem. Res. 57 (20) (2018) 6821–6829, https://doi.org/10.1021/acs.iecr.8b00230.

[13] J. Niu, H. Liu, Y. Jin, B. Fan, W. Qi, J. Ran, Comprehensive review of Cu-based CO2 hydrogenation to CH3OH: insights from experimental work and theoretical analysis, Int. J. Hydrogen Energy 47 (15) (2022) 9183–9200, https://doi.org/ 10.1016/j.ijhydene.2022.01.021.

[14] J. Wang, et al., A highly selective and stable ZnO-ZrO2 solid solution catalyst for CO2 hydrogenation to methanol, Sci. Adv. 3 (10) (2017) 1–11, https://doi.org/ 10.1126/sciadv.1701290.

[15] X. Zhang, et al., Highly dispersed ZnO sites in a ZnO/ZrO_2 catalyst promote the CO_2-to-methanol reaction 202416899 (2025), https://doi.org/10.1002/ange.202416899.

[16] H. Chang, et al., Unlocking methanol synthesis from CO2 and H2 on ZnO/ZrO2 catalysts: surface hydroxyl-mediated activation, ACS Catal. (2025) 6005–6017, https://doi.org/10.1021/acscatal.5c01585.

[17] E. Kianfar, S. Hajimirzaee, S. mousavian, A.S. Mehr, Zeolite-based catalysts for methanol to gasoline process: a review, Microchem. J. 156 (September 2019) (2020) 104822, https://doi.org/10.1016/j.microc.2020.104822.

[18] S. Biswas, T. Pal, Supported Metal and Metal Oxide Particles with Proximity Effect for Catalysis, 2020, pp. 35449–35472, https://doi.org/10.1039/d0ra06168a.

[19] J. Zecevic, G. Vanbutsele, K.P. De Jong, J.A. Martens, Nanoscale intimacy in bifunctional catalysts for selective conversion of hydrocarbons, Nature 528 (7581) (2015) 245–254, https://doi.org/10.1038/nature16173.

[20] N. Martín, et al., MOF-derived/zeolite hybrid catalyst for the production of light olefins from CO2, ChemCatChem 12 (22) (2020) 5750–5758, https://doi.org/ 10.1002/cctc.202001109.

[21] H. Jiang, Z. Hou, Y. Luo, A Kinetic View on Proximity-Dependent Selectivity of Carbon Dioxide Reduction on Bifunctional Catalysts, 2020, https://doi.org/ 10.1021/acscatal.0c03414.

[22] O. Parra, A. Portillo, J. Erena, A.T. Aguayo, J. Bilbao, A. Ateka, Boosting the ˜ activity in the direct conversion of CO2/CO mixtures into gasoline using ZnO-ZrO2 catalyst in tandem with HZSM-5 zeolite, Fuel Process. Technol. 245 (January) (2023), https://doi.org/10.1016/j.fuproc.2023.107745.

[23] J.L. Weber, N.A. Krans, J.P. Hofmann, E.J.M. Hensen, J. Zecevic, P.E. De Jongh, Effect of proximity and support material on deactivation of bifunctional catalysts for the conversion of synthesis gas to olefins and aromatics, Catal. Today 342 (January 2019) (2020) 161–166, https://doi.org/10.1016/j.cattod.2019.02.002.

[24] Y. Ding, et al., Effects of Proximity-Dependent Metal Migration on Bifunctional Composites Catalyzed Syngas to Olefins, 2021, https://doi.org/10.1021/ acscatal.1c01649.

[25] J. Lyu, S. Yu, Z. Peng, J. Zhou, Z. Liu, X. Li, Control of the proximity of bifunctional zeolite @Al2O3 catalysts for efficient methanol conversion into hydrocarbons 406 (March) (2022) 82–91, https://doi.org/10.1016/j.cattod.2022.07.017.

[26] S. Chen, J. Wang, Z. Feng, Y. Jiang, H. Hu, Y. Qu, Hydrogenation of CO2 to Light Olefins over ZnZrOx/SSZ-13 Angewandte 730000 (2024), https://doi.org/ 10.1002/anie.202316874.

[27] X. Wang, et al., Macroscopic assembly style of catalysts significantly determining their efficiency for converting CO2 to gasoline, Cat. Sci. Technol. 9 (19) (2019) 5401–5412, https://doi.org/10.1039/c9cy01470e.

[28] A. Dokania, et al., Designing a multifunctional catalyst for the direct production of gasoline-range isoparaffins from CO2, JACS Au 1 (11) (2021) 1961–1974, https:// doi.org/10.1021/jacsau.1c00317.

Published in : Chemical Engineering Journal (2025), vol. 523
DOI: 10.1016/j.cej.2025.167966
Status : Postprint (Author's version)

[29] Z. Li, et al., Highly selective conversion of carbon dioxide to aromatics over tandem catalysts, Joule 3 (2) (2019) 570–583, https://doi.org/10.1016/j.joule.2018.10.027.
[30] O. Parra, A. Portillo, J. Erena, J. Bilbao, A. Ateka, Production of isoparaffinic gasoline from CO2/CO over ZnO-ZrO2/nano-sized HZSM-5 tandem catalyst, Catal. Today 458 (December 2024) (2025), https://doi.org/10.1016/j.cattod.2025.115397.
[31] S. Ghosh, L. Olsson, D. Creaser, Methanol mediated direct CO2 hydrogenation to hydrocarbons: experimental and kinetic modeling study, Chem. Eng. J. 435 (P3) (2022) 135090, https://doi.org/10.1016/j.cej.2022.135090.
[32] Y. Wang, et al., Visualizing element migration over bifunctional metal-zeolite catalysts and its impact on catalysis, Angew. Chemie 133 (32) (2021) 17876–17884, https://doi.org/10.1002/ange.202107264.
[33] I. Khalil, K. Thomas, H. Jabraoui, P. Bazin, F. Maug´e, Selective elimination of phenol from hydrocarbons by zeolites and silica-based adsorbents—impact of the textural and acidic properties, J. Hazard. Mater. 384 (July 2019) (2020) 121397, https://doi.org/10.1016/j.jhazmat.2019.121397.
[34] C.A. Emeis, Cheminform abstract: determination of integrated molar extinction coefficients for IR absorption bands of pyridine adsorbed on solid acid catalysts, ChemInform 24 (38) (1993), https://doi.org/10.1002/chin.199338056.
[35] J. Alirio, et al., Support effects in vanadium incipient wetness impregnation for oxidative and non-oxidative propane dehydrogenation catalysis, Catal. Today 430 (January) (2024) 114546, https://doi.org/10.1016/j.cattod.2024.114546.
[36] J. Devos, A. Sajid, C. Aelbers, M. Dusselier, Parallel-consecutive CO formation during CO2 hydrogenation to olefins in a tandem ZnZrOx/SSZ-13, ACS Sustain. Chem. Eng. (2025), https://doi.org/10.1021/acssuschemeng.5c01336.
[37] F. Brandi, et al., The role of Beta zeolites in the selective single O-demethylation of alkyl-syringols to alkyl-methoxycatechols, a novel polymer building block class, Green Chem. (2025), https://doi.org/10.1039/d4gc04824e.
[38] M. Westgård Erichsen, S. Svelle, U. Olsbye, The influence of catalyst acid strength on the methanol to hydrocarbons (MTH) reaction, Catal. Today 215 (2013) 216–223, https://doi.org/10.1016/j.cattod.2013.03.017.
[39] R. Gounder, E. Iglesia, Catalytic consequences of spatial constraints and acid site location for monomolecular alkane activation on zeolites, J. Am. Chem. Soc. 131 (5) (2009) 1958–1971, https://doi.org/10.1021/ja808292c.
[40] A. Vimont, F. Thibault-Starzyk, M. Daturi, Analysing and understanding the active site by IR spectroscopy, Chem. Soc. Rev. 39 (12) (2010) 4928–4950, https://doi. org/10.1039/b919543m.
[41] J.P. Marques, et al., Dealumination of HBEA zeolite by steaming and acid leaching: distribution of the various aluminic species and identification of the hydroxyl groups, Comptes Rendus Chim. 8 (3–4) (2005) 399–410, https://doi.org/10.1016/ j.crci.2005.01.002.
[42] I.C. Medeiros-Costa, E. Dib, N. Nesterenko, J.P. Dath, J.P. Gilson, S. Mintova, Silanol defect engineering and healing in zeolites: opportunities to fine-tune their properties and performances, Chem. Soc. Rev. 50 (19) (2021) 11156–11179, https://doi.org/10.1039/d1cs00395j.
[43] P. Arudra, T.I. Bhuiyan, M.N. Akhtar, A.M. Aitani, S.S. Al-Khattaf, H. Hattori, Silicalite-1 as efficient catalyst for production of propene from 1-butene, ACS Catal. 4 (11) (2014) 4205–4214, https://doi.org/10.1021/cs5009255.
[44] R. Gounder, E. Iglesia, The catalytic diversity of zeolites: confinement and solvation effects within voids of molecular dimensions, Chem. Commun. 49 (34) (2013) 3491–3509, https://doi.org/10.1039/c3cc40731d.
[45] R. Rungsirisakun, T. Nanok, M. Probst, J. Limtrakul, Adsorption and diffusion of benzene in the nanoporous catalysts FAU, ZSM-5 and MCM-22: a molecular dynamics study, J. Mol. Graph. Model. 24 (5) (2006) 373–382, https://doi.org/ 10.1016/j.jmgm.2005.10.003.
[46] J. Zhang, et al., Hydrogen transfer versus olefins methylation: on the formation trend of propene in the methanol-to-hydrocarbons reaction over Beta zeolites, J. Catal. 368 (2018) 248–260, https://doi.org/10.1016/j.jcat.2018.10.015.
[47] K. Lee, S. Lee, Y. Jun, M. Choi, Cooperative effects of zeolite mesoporosity and defect sites on the amount and location of coke formation and its consequence in deactivation, J. Catal. 347 (2017) 222–230, https://doi.org/10.1016/j.jcat.2017.01.018.
[48] H. Schulz, 'Coking' of zeolites during methanol conversion: basic reactions of the MTO-, MTP- and MTG processes, Catal. Today 154 (3–4) (2010) 183–194, https:// doi.org/10.1016/j.cattod.2010.05.012.
[49] P.L. Benito, A.G. Gayubo, T. Aguayo, Deposition and Characteristics of Coke over a H-ZSM5 Zeolite-Based Catalyst in the MTG Process, 1996, pp. 3991–3998.
[50] S.S. Arora, D.L.S. Nieskens, A. Malek, A. Bhan, Lifetime improvement in methanol- to-olefins catalysis over chabazite materials by high-pressure H2 co-feeds, Nat. Catal. 1 (9) (2018) 666–672, https://doi.org/10.1038/s41929-018-0125-2.
[51] P. Sharma, J. Sebastian, S. Ghosh, D. Creaser, L. Olsson, Recent advances in hydrogenation of CO2into hydrocarbonsviamethanol intermediate over heterogeneous catalysts, Cat. Sci. Technol. 11 (5) (2021) 1665–1697, https://doi. org/10.1039/d0cy01913e.
[52] F. Mirshafiee, R. Khoshbin, R. Karimzadeh, A green approach for template free synthesis of Beta zeolite incorporated in ZSM-5 zeolite to enhance catalytic activity in MTG reaction: effect of seed nature and temperature, J. Clean. Prod. 361 (May) (2022) 132159, https://doi.org/10.1016/j.jclepro.2022.132159.
[53] A.G. Gayubo, A.T. Aguayo, A.L. Moran, M. Olazar, J. Bilbao, Role of water in the kinetic modeling of catalyst deactivation in the MTG process, AIChE J. 48 (7) (2002) 1561–1571, https://doi.org/10.1002/aic.690480718.